Extrinsic Signatures Embedding and Detection in Electrophotographic Halftone Images through Laser Intensity Modulation

Pei-Ju Chiang[1], Aravind K. Mikkilineni[2], Edward J. Delp[2], Jan P. Allebach[2] and George T.-C. Chiu[1]; School of Mechanical Engineering[1], School of Electrical and Computer Engineering[2], Purdue University; West Lafayette, Indiana/USA

Abstract

In this paper, we demonstrated the feasibility of embedding unperceivable code sequence by modulating dot gains through laser intensity modulation for halftone images. From a communication systems point of view, a printer and a document scanner form the physical layer of a communication channel, where information can be hidden in halftone images and reliably transmitted and extracted. In the proposed approach, we will leverage our previous results in embedding unperceivable banding signals to halftone images and develop an integrated embedding and detection algorithm to embed and extract information with high payload capacity. Specifically, we will characterize the embedding capacity and detection rate associated with the proposed algorithm. Preliminary experimental results will be presented.

Introduction

Printed material is a direct accessory to many criminal and terrorist acts. The ability to identify the device or type of device to print the material in question and the authentication of the printed material would provide a valuable aid for law enforcement and intelligence agencies.

To identify the printing device or authentication of the document, intrinsic signatures [1-7] and extrinsic signatures [8-11] of printers have been investigated. Intrinsic signatures involve tracing the intrinsic features in the printout that are characteristic of that particular printer, model or manufacture's products. Extrinsic signatures are specific information embedded into the printed document through modulating the printing process parameters. In our previous work, we have presented the techniques of modulating the exposure of the electrophotographic (EP) process through laser intensity modulation to embed unperceivable banding into half-toned images [9]. We have proposed embedding and decoding techniques for text documents without image quality degradation [8,10,12]. For half-toned images, we have proposed to embed multiple frequency banding signals and apply DFT to extract the embedded signals [11]. Sine the resolution of DFT depends on the extracted data length, the approach proposed in [11] will constrain the applicable image size and decoding performance. In this work, we propose improved embedding and detection algorithms for half-toned images to increase the payload capacity.

Since the embedded data can be extracted from images with different gray-level and from anywhere of the image, its exact phase configuration within the image is lost. To retrieve the embedded code, we exploit the properties of pseudo-random binary sequence (PRBS) or pseudo-random noise (PN) sequences to develop our embedding and detection algorithms. To embed extrinsic signatures without image quality degradation and human perception, we modulate the embedded code to higher frequency band according to the previous results in embedding unperceivable banding signal [9]. An HP color laserjet 4500 is used as the experimental platform for this study.

This paper is organized as follows. The embedding and detection algorithms for half-toned images without human perception will be discussed in the next section followed by the presentation and discussion of preliminary experimental results. The conclusions are given in the last section.

Information Embedding and Extraction

The process of embedding and decoding extrinsic signatures in halftone images is outlined in Fig. 1. Through modulating the laser intensity, a specific PN sequence is embedded in a half-toned image. After scanning the printed image by a calibrated scanner, the scanned image is projected to the process direction to obtain a 1-D data sequence. After normalization, correlation between the data sequence and the set of all possible PN sequences is applied to identify the sequence with the maximum correlation value. Different segments from the same printed image are extracted and processed, a majority vote from all the extracted images of its correlated PN sequence will determine the embedded sequence.

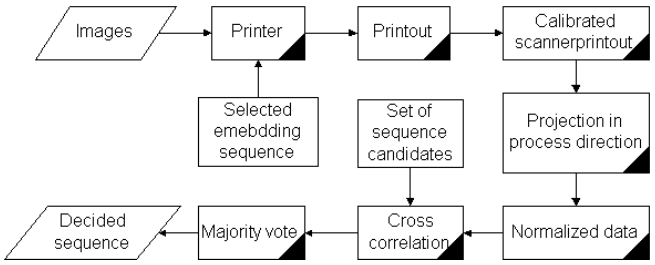

***Figure 1**. Process block diagram for embedding and decoding extrinsic signatures of halftone images*

Encoding and Embedding Algorithm: Pseudo-Random Binary Noise Sequence

In this section we will propose a coding and embedding algorithm to embed a unique sequence repeatedly along the process direction of a half-toned image. We do not assume prior knowledge of the image content, which implies that the relative phase information of the extracted image sample with respect to the original code is unknown. A binary PN sequence is one

possible solution to avoid the lack of synchronization between the detector and the encoder [12]. In this work, the *Gold sequence* [12], which is one type of binary PN sequences, will be used. An n-bit Gold sequence has the following properties:

- Period $T = 2^n - 1$
- $2^n + 1$ different sequences in one code set
- Cross-correlation values take on the same 3 values for each pair of sequences, which are -1, $t(n) - 2$ and $-t(n)$, where $t(n) = 1+2^{[(n+2)/2]}$

However, the printed image will not be able to present each element of sequence precisely due to the limited MTF of the printer. For example, if the sequence is {1 1 –1 1 1}, then –1 will not be printed clearly because the resolution of the printer is limited and the dot that represents of the element –1 will be overlapped by its neighbor dots. To reduce this effect, each element in each sequence is repeated T_s times. For example, {1 –1 1} is expanded to {1 1 –1 –1 1 1} for $Ts = 2$. Therefore, the total length of each sequence becomes $Ts \cdot T$. For instance, if $n = 5$, we will have 33 different sequences, that means we have 33 different candidates to embed signal into the image. If we repeat each element of the selected sequence $T_s = 5$ times, we need at least $Ts \cdot T = 5 \cdot 31 = 155$ scan-lines to represent one period of the sequence. Table 1 shows the numbers of scan-line we need to represent one period of the sequence for different n and Ts. The right column of the table represents the number of sequence candidates based on the selection of n. From a payload capacity point of view, it is desirable to have reliable detection using the shortest extracted data length, i.e. smallest number of scan-lines. There is obviously a trade-off between the required data sequence length and the reliability of detection. Note to preserve the desired PN sequence property, n cannot be too small.

Table 1: Required extracted data length and number of sequence candidates for a Gold sequence

*Ts*T (scan-lines)*	*Ts=1*	*Ts=3*	*Ts=5*	*Number of sequence candidates*
n=5	*31*	*93*	*155*	*33*
n=6	*63*	*189*	*315*	*65*
n=7	*127*	*381*	*635*	*129*

Since the Gold sequence is a binary sequence, its spectrum is a sinc function with bandwidth depending on T_s. Here we define the elements in one Gold sequence to be $[x_1, \ldots, x_{2^n-1}]$. Based on the laser intensity modulation threshold developed in [9], high spatial frequency region provides a larger range of intensity modulation while staying below the human perception threshold. Therefore, to exploit the larger modulation range at higher spatial frequency, the actual embedded sequence code $X(l)$ is the product of the original PN code sequence x_i with a high spatial frequency carrier signal, which can be presented as

$$X(l) = \sum_{i=0}^{T-1} x_i 1(l - iT_s) \sin(2\pi F_s (l - iT_s)/R_p) \quad (1)$$

where F_s is the modulation frequency and R_p is the resolution of the printer. The embedded sequence $X(l)$ is then embedded into the half-toned image by a channel coder matching the binary value to a appropriately selected laser intensity. A typical code is to match the value 1 with the maximum allowable intensity and the value –1 to the minimal allowable intensity.

Detection Algorithm

To detect the embedded signal, a scanned image is first segmented into many sub-images. Let N_m represents the set of sub-images in the m_{th} image and X^*_{mn} represents the extracted data from the n_{th} sub-images of the m_{th} image and let the sequence candidates be X_k, where k is the index of the sequences indexed from 1 to 2^n+1. The correlation between sequence candidates X_k and extracted data X^*_{mn} can be presented as:

$$\rho^k_{mn} = \max_{l=1\sim TsT} \frac{X^*_{mn} \cdot X_k(l)}{\left|X^*_{mn}\right| \left|X_k(l)\right|}$$

For each image m, we count the percentages of sub-images with greatest maximum correlation value with sequence candidate X_k can be written as

$$P^k_m = \frac{1}{|N_m|} \sum_{\substack{n \in N_m \\ i=1\sim 2^n+1}} 1(\rho^k_{mn} \geq \rho^i_{mn})$$

The decoded sequence for image m , X_m ,is estimated by choosing the sequence with the maximum percentage $P_m{}^k$, i.e.

$$X_m = X_k, \quad \text{if } P^k_m \geq P^i_m, \quad i = 1 \sim 2^n + 1$$

To measure the overall performance of this embedding and detection algorithm, the percentage of sub-images in all the images that has its maximum correlation value corresponding to the actual encoded sequence X_* is calculated as

$$P^* = \sum_{i=1}^{M} P^*_i \quad (2)$$

where M is the total number of printed images. The majority vote result P, which represents the percentages of images that are decoded correctly can be calculated as

$$P = \frac{1}{M} \sum_{m=1}^{M} 1(X_m = X_*) \quad (3)$$

Experimental Results

To test the algorithms we proposed in last section, a test page with 50% gray filled image is used and printed with the printer's default halftone. Each test page is printed 5 times. In this work, a 5 bit ($n = 5$) PN sequence is used with the embedded sequence indexed as sequence 1. To determine an appropriate T_s value as shown in Table 1, the P^1 values, see Eq. (2), are measured for different T_s with modulation amplitude $\Delta V = 0.1V$ and the results are shown in Table 2. From Table 2, we can see that when T_s increases, the percentage P^1 of sub-images with maximum correlation value with sequence 1 also increases. Therefore, as mentioned in last section, there is a trade-off between detection rate and T_s, i.e., data length. For $T_s = 5$, the corresponding detection rate is high and the required data length, 155 scan-lines, is about a quarter of an inch at 600 dpi printer resolution. For the subsequent experiments, $T_s = 5$ will be used. Note that for this coding sequence, the theoretical maximum payload capacity is about 20 bits per inch. Of course, the achievable and reliable payload capacity will be less.

Table 3 shows the detection rate P^1 for different modulation amplitudes ΔV. It is obvious to note that higher modulation amplitude implies higher energy of the embedding signal that will translates to higher detection rate.

Although with high detection rate, the square gratings associated with the PN sequence is visible even with modulation amplitude that is fall below the human visual threshold. As discussed in the previous section, one possible solution to reduce the visibility of the embedded code is to modulate the sequence to higher spatial frequencies, see Eq. (1). Table 4 shows the detection rate P^1 of the modulated code sequence where the original code is modulated to spatial frequencies 60 and 120 cycles per inch, respectively. From Table 4, the detection rate decreases as the modulation frequency increase because of the limited MTF of the printing system. However, with 33 candidate sequences, 46.86% of the extracted data voted for sequence 1, the correct choice, is a sufficient high percentage. Figure 2 shows the P^k values for all the 33 candidate sequences. From Fig. 2, except for sequence 1, none of the other 32 sequences received more than 5% of the vote, with an average voting rate of 100/33=3.03% that is associated with an uncorrelated noise sequence.

Table 5 shows the majority vote result P for the two modulation frequencies and two modulation amplitude ΔV =0.1/0.05 [V], respectively. As can be seen, the majority vote result are 5 votes out of 5 images for both modulation frequencies at the modulation amplitude of 0.1 volt. Figures 3 and 4 compare a un-modulated printed image with one that is printed with a coded sequence with a modulation frequency of 120 cycles/in and laser intensity modulation of 0.1 volt. Comparing Figures 3 and 4, there are no visible degradation of image quality or visible indication of an coded message.

Table 2: Percentage P^k values for different Ts with k=1, n=5 and ΔV=0.1V

P^1	T_s=1	T_s=3	T_s=5
n=5	1.14%	91.38%	96.57%

Table 3: Percentage P^k values for different ΔV with k=1, n=5, and T_s=5

P^1	ΔV=0.1(V)	ΔV=0.05(V)	ΔV=0.025(V)
n=5, T_s=5	96.57%	40.57%	5.71%

Table 4: Percentage P^k for different ΔV and F_s with k=1, n=5, and T_s=5

P^1	F_s=60 (cycles/in)	F_s=120 (cycles/in)
ΔV=0.1 (V)	86.86%	46.86%
ΔV=0.05 (V)	20%	8%

Table 5: Majority vote result P for different ΔV and F_s with k=1, n=5, and T_s=5

P	F_s=60 (cycles/in)	F_s=120 (cycles/in)
V=0.1 (V)	100%	100%
V=0.05 (V)	80%	20%

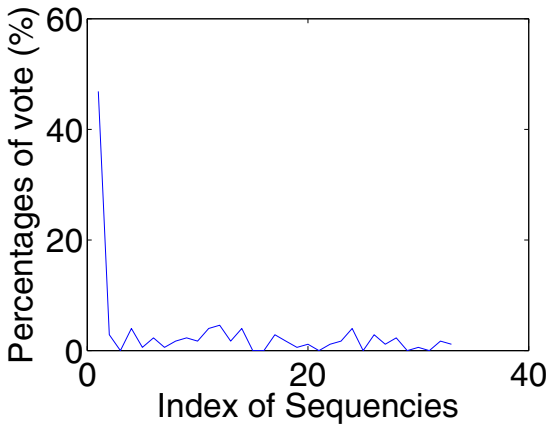

***Figure 2**. Percentage of votes for the 33 candidate sequences*

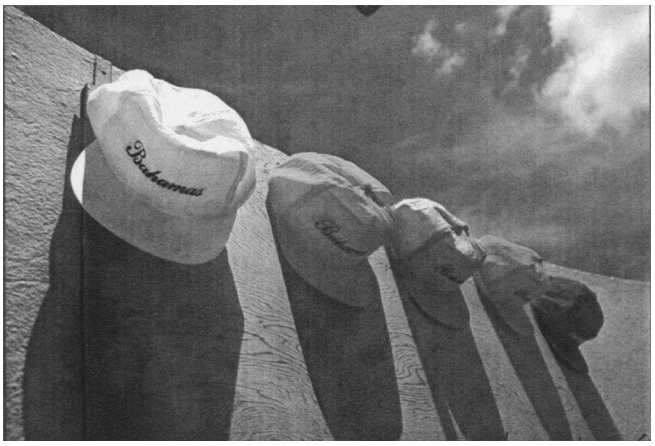

***Figure 3**. Printed image without any modulation*

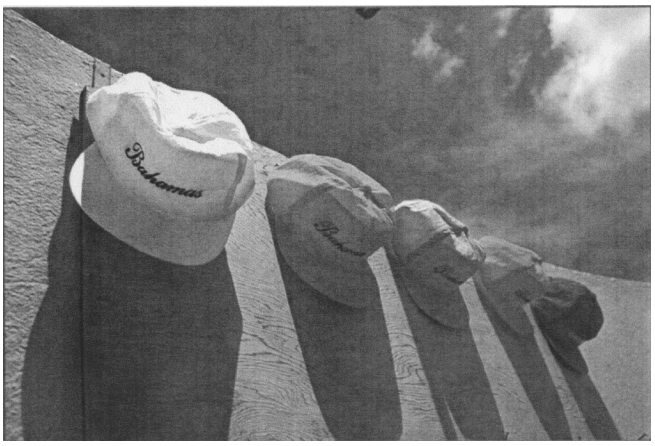

***Figure 4**. Printed image modulated with ΔV=0.1, F_s=120 cycles/in, n=5 and T_s=5*

Conclusions

We have demonstrated the feasibility to embed and extract binary PN sequences into half-toned images without visible image degradation. No a priori information of the original image is required, nor is synchronization needed during decoding. A theoretical maximum payload capacity can be predicted with the proposed methods. Repeatedly embedding the same code sequence

through out the image can avoid cropping attack at the expense of payload capacity. We are currently investigating the robustness of the proposed embedding and detection algorithms with different consumables and operating environment.

Acknowledgement

The authors would like to acknowledge the support of the National Science Foundation under the grant CCR-0524540.

References

[1] G. N. Ali, P.J. Chiang, A. K. Mikkilineni, J. P. Allebach, G. T. C. Chiu and E. J. Delp, "Intrinsic and Extrinsic Signatures for Information Hiding and Secure Printing with Electrophotographic Devices", in *Proceedings of the IS&T's NIP19: International Conference on Digital Printing Technologies*, p511-515, 2003.

[2] G. N. Ali, A. K. Mikkilineni, P. J. Chiang, J. P. Allebach, G. T. C. Chiu and E. J. Delp, "Application of Principal Components Analysis and Gaussian Mixture Models to Printer Identification", in *Proceedings of the IS&T's NIP20: International Conference on Digital Printing Technologies*, p301-305, 2004.

[3] A. K. Mikkilineni, P. J. Chiang, G. N. Ali, G. T. C. Chiu, J. P. Allebach, and E. J. Delp, "Printer Identification Based on Textural Features", in *Proceedings of the IS&T's NIP20: International Conference on Digital Printing Technologies*, p306-311, 2004.

[4] A. K. Mikkilineni, G. N. Ali, P.J. Chiang, G. T. C. Chiu, J. P. Allebach, and E. J. Delp, "Signature-embedding in printed documents for security and forensic applications", in *Proceedings of the SPIE International Conference on Security, Steganography, and Watermarking of Multimedia Contents VI*, p. 455-466, Jun 22 2004.

[5] A. K. Mikkilineni, O. Arslan, P. J. Chiang, R. M. Kumontoy, J. P. Allebach, G. T.-C. Chiu and E. J. Delp, "Printer Forensic Using SVM Techniques", in *Proceedings of the IS&T's NIP21: International Conference on Digital Printing Technologies*, p223-226, 2005.

[6] A. K. Mikkilineni, P. J. Chiang, G. N. Ali, G. T. C. Chiu, E. J. Delp and J. P. Allebach, "Printer Identification Based on Graylevel Co-occurrence features for Security and Forensic Applications", in *Proceedings of the SPIE International Conference on Security, Steganography, and Watermarking of Multimedia Contents VII*, vol. 5681, p430-440, 2005.

[7] O. Arslan, R. M. Kumonotoy, P.J. Chiang, A.K. Mikkilineni, J. P. Allebach, G. T. C. Chiu and E. J. Delp, "Identification of Inkjet Printers for Forensic Applications", in *Proceedings of the IS&T's NIP21: International Conference on Digital Printing Technologies*, p235-238, 2005.

[8] A. K. Mikkilineni, P. J. Chiang, S. Suh, G. T. C. Chiu, J. P. Allebach and E. J. Delp, "Information embedding and extraction for electrophotographic printing processes", *Proceedings of the SPIE International Conference on Security, Steganography, and Watermarking of Multimedia Contents VIII*, vol. 6072, p385-396, 2006.

[9] P. J. Chiang, G. N. Ali, A. K. Mikkilineni, E. J. Delp, J. P. Allebach, and G. T.C. Chiu, "Extrinsic Signatures Embedding Using Exposure Modulation for Information Hiding and Secure Printing in Electrophotography", in *Proceedings of the IS&T's NIP20: International Conference on Digital Printing Technologies*, p295-300, 2004.

[10] P. J. Chiang, Mikkilineni, O. Arslan, R.M. Kumontoy, G. T.C. Chiu , E. J. Delp and J. P. Allebach, "Extrinsic Signatures Embedding in Text Document Using Exposure Modulation for Information Hiding and Secure Printing in Electrophotography", in *Proceedings of the IS&T's NIP21: International Conference on Digital Printing Technologies*, p231-234, 2005.

[11] P. J. Chiang, G. N. Ali, A. K. Mikkilineni, E. J. Delp, J. P. allebach and G. T. C. Chiu, "Extrinsic Signatures Embedding and Detection for Information Hiding and Secure Printing in Electrophotography" , in *Proceedings of the 2006 American Control Conference*, p 2539-2544, Jun 2006.

[12] Michael B. Pursley, Introduction to Digital Communications, 2005 Pearson Education, Inc.

Author Biography

Pei-Ju Chiang received her B.S. degree in Mechanical and Marine Engineering from the National Taiwan Ocean University, in 1999 and a M.S. degree in Mechanical Engineering from the National Central University in 2001. She is currently pursuing her Ph.D. degree in the School of Mechanical Engineering at Purdue University. Her research interests are securing documents, modeling and analysis of digital printing and imaging processes.